Direct NMR Evidence of Phase Solitons in the Spin Ground State of Overdoped Manganites

D. Koumoulis,[1] N. Panopoulos,[1] A. Reyes,[2] M. Fardis,[1] M. Pissas,[1] A. Douvalis,[3] T. Bakas,[3] D. N. Argyriou,[4] and G. Papavassiliou[1,*]

[1]*Institute of Materials Science, NCSR, Demokritos, 153 10 Aghia Paraskevi, Athens, Greece*
[2]*National High Magnetic Field Laboratory, Tallahassee, Florida 32310, USA*
[3]*Physics Department, University of Ioannina, P.O. Box 1186, 451 10 Ioannina, Greece*
[4]*Helmholtz-Zentrum Berlin fuer Materialen und Energy, Hahn-Meitner Platz 1, D-14109 Berlin, Germany*

(Received 23 November 2009; published 19 February 2010)

Charge ordering phenomena in overdoped $La_{1-x}Ca_xMnO_3$ (LCMO) manganites with $x \geq 0.5$ are generally believed to be associated with the formation of charge stripes composed of alternating Mn^{3+} and Mn^{4+} charges. However, a number of recent experiments indicate that instead of stripes the charge in these systems is spatially organized in a uniform charge density wave. At the same time theory predicts that the ground state is modulated by an incommensurate (IC) orbital and charge soliton lattice. Here, by using nuclear magnetic resonance we provide the first direct evidence that the spin ground state in overdoped LCMO manganites is IC modulated with phase solitons. At higher temperatures the solitonic superstructure is replaced by a uniform spin-density wave, subjected to coherent slow fluctuations, showing a striking similarity with slow fluctuations in the striped phase of high T_c cuprates and nickelates.

DOI: 10.1103/PhysRevLett.104.077204 PACS numbers: 75.47.Lx, 75.30.Fv, 75.47.Gk, 76.60.−k

Hole doped transition metal oxides are famous due to their extraordinary electron transport properties, such as high temperature superconductivity (cuprates) and colossal magnetoresistance (manganites) [1]. Astonishingly, the parent system of these compounds is an antiferromagnetic (AFM) Mott insulator [2], whereas an important role in their transport properties is played by the way that holes are self-organized with doping [2–5]. Both experiments and theory have shown that when adding holes the homogeneous insulating phase breaks into AFM regions, which are separated by hole-rich clumps (stripes) with a rapid change of the phase of the background spins and orbitals [2,5–7]. This behavior has been assigned to the competition between the underlying AFM and Coulomb interactions, which favor charge localization, and the zero-point kinetic energy of the added holes, which tends to delocalize charge. Evidently, the appearance of charge stripes in AFM transition metal oxides is conjugate with a spin and orbital modulation.

The formation of an incommensurate (IC) spin-density wave (SDW) associated with charge stripes was first observed in superconducting $La_{2-x}Sr_xCuO_4$ and their insulating nickelate counterparts [8,9]. Specifically, inelastic neutron scattering experiments have shown that holes in these materials tend to localize into periodically arranged antiphase domain walls, i.e., walls where the phase of the AFM order shifts by π, which propagate diagonally through the CuO_2 (respectively, NiO_2) layers [2]. At the same time, the formation of stripes is accompanied by a strong wipeout effect of the NMR and nuclear quadrupole resonance signal over an extended temperature range, which declares a significant slowing down of the spin and charge fluctuations [10–12]. This is in accordance with the idea that the stripe phase is a slow fluctuating strongly correlated fluid [2], which gradually freezes by cooling [12].

In the case of overdoped (also called electron-doped) $La_{1-x}Ca_xMnO_3$ (LCMO) manganites for $x \geq 0.5$, charge ordering phenomena have been viewed with a similar rationale. Electron diffraction experiments unveiled an IC charge modulation with a wave vector parallel to the reciprocal lattice vector $q \parallel a^\star$ [13–15], associated with orbital and AFM spin ordering [5]. This charge modulation has been considered as a signature of charge stripes arising from the ordered arrangement of alternating Mn^{+3} and Mn^{+4} ions. However, a number of recent experiments [16,17] and theoretical calculations [18,19] put into question this kind of Mn^{+3} and Mn^{+4} charge alternation, while other works indicate the formation of a charge modulation wave with a uniform periodicity for all $x \geq 0.5$ [20–22]. A collective sliding of the charge system in a moderate electric field was also reported at half-doping, $x = 0.5$ [23]. These results have been interpreted in the framework of a charge-density wave (CDW) model [22,24] with nonzero and possibly high itineracy. Recently, it has been also proposed that the nanoscale spin and orbital texture observed in overdoped manganites is explainable in the framework of an IC solitonic ground state [25,26], which is produced by orbital solitons carrying charge equal to $\pm e/2$ [26]. However, no experimental evidence about the existence of orbital or spin solitons has been reported so far; only a uniform IC modulation has been detected in overdoped LCMO for $T \geq 90$ K [20]. Here, by using ^{139}La NMR in magnetic field 4.7 T, we provide clear evidence about the formation of a uniform IC spin modulation in overdoped LCMO manganites, which becomes visible for $T < 30$ K. Most importantly, at very low temperatures this modulation is shown to split into regularly arranged com-

mensurate and narrow IC (soliton) regions, pointing at an IC soliton-modulated SDW as $T \rightarrow 0$.

Until now, the most detailed information about charge, spin, and orbital modulated phases in doped AFM transition metal oxide compounds has been acquired by neutron and electron scattering techniques [3,14]. Diffraction of a neutron or electron beam by long-period spin- and charge-density modulations yields satellite Bragg peaks, which provide information about the spatial period and orientation of the corresponding modulation, whereas the intensity provides a measure of the modulation amplitude. A complementary and equally powerful technique in the study of modulated structures is NMR. In the past, NMR has been successfully applied in the study of structural IC phases [27], as well as CDW [28] and SDW systems [29]. The ability of NMR to provide information about the appearance and evolution of an IC spin modulation is clearly demonstrated in Fig. 1.

Assuming a 1D SDW, the modulation wave varies in space according to the formula $\rho = A\cos(\varphi(x))$ [22,24]. In magnetic systems the NMR frequency is proportional to the local hyperfine field $B_{\mathrm{hf}} = (1/\gamma\hbar)C\langle S\rangle$ (C is the hyperfine coupling constant and $\langle S\rangle$ is the average electron spin probed by the resonating nuclei [30]); hence, the NMR frequency will be accordingly modulated, $\nu = \nu_0 + \nu_1\cos(\varphi(x))$. This gives rise to a characteristic NMR frequency distribution depicted by the formula, $f(\nu) \propto \frac{1}{\nu_1|\sin(\varphi)(d\varphi/dx)|}$ [27]. In the case of an IC modulation, the phase of the modulation wave $\varphi(x)$ varies in space according to the sine-Gordon (SG) equation, $\frac{d^2\varphi}{dx^2} = w\sin(m\varphi(x))$ [24,31,32], where m is a commensurability factor defining the crystal symmetry [24,31], and w is a constant depending on the electronic properties of the system and the amplitude of the modulation wave [24,32]. Figure 1 presents the spatial variation of $\varphi(x)$ by solving the SG equation for two cases: (i) a nearly plane wave IC modulation with $w \ll 1$ (left middle panel) and (ii) an IC solitonic phase modulation with $w \leq 1$ (left upper panel). The commensurability factor was set equal to $m = 1$, in accordance with theoretical studies for 1D CDWs [32]. This gives a phase shift across solitons equal to $\Delta\varphi = 2\pi$. Other works predict $\Delta\varphi = \pm\pi/2$ and a fractional charge $\pm e/2$ [26], while in systems with coexisting charge and spin order a change in phase equal to $\pm\pi$ has been predicted, even in the presence of higher order commensurability (e.g., $m = 3$ or 4) [33]. For reasons of comparison a commensurate modulation with constant phase $\varphi(x)$ is also presented in the left lower panel of Fig. 1, which corresponds to spin configuration with the crystal-lattice periodicity. Simulated NMR spectra for the three cases (with initial phase $\varphi_0 = \pi/2$ for the modulation wave) are presented in the right-hand panels of Fig. 1. Evidently, in the case that the system undergoes a series of commensurate → IC (plane wave) → IC (solitonic) phase transitions, the NMR signal is expected to transform from a narrow symmetric line shape in the commensurate phase to a broad frequency distribution in the IC plane wave limit, and finally to the composite signal of the right upper panel. This is exactly what we have observed in the temperature variation of the ^{139}La NMR spectra in overdoped LCMO manganites.

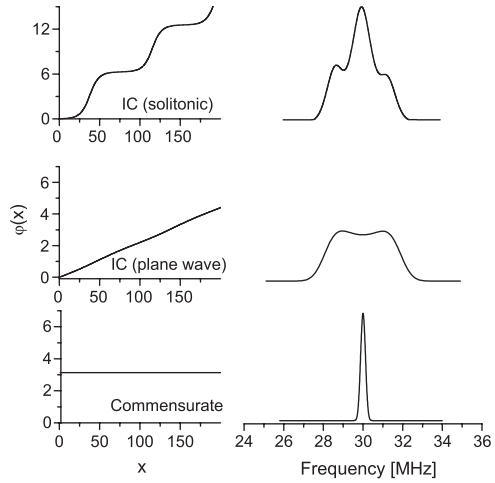

FIG. 1. The spatial variation of the phase $\varphi(x)$ of a SDW and the corresponding NMR line shapes for three different cases. (i) A spin modulation with constant phase $\varphi(x)$ (lower panel), corresponding to a commensurate spin configuration with the crystal-lattice periodicity. (ii) An IC plane wave phase modulation (middle panel). (iii) An IC modulation with phase solitons (upper panel).

Experiments were performed on polycrystalline $La_{1-x}Ca_xMnO_3$ samples for $x = 0.5$, 0.55, 0.66, 0.63, and 0.69, prepared by thoroughly mixing high purity stoichiometric amounts of $CaCO_3$, La_2O_3, and MnO_2. The mixed powders prepared in pastile form reacted in air at 1400 °C for several days with intermediate grinding and then slowly cooled down to room temperature. X-ray diffraction measurements were performed on a D500 SIEMENS diffractometer, showing that all samples are single phase materials with very good crystallinity. In addition, samples were magnetically characterized on a Quantum Design SQUID magnetometer. The NMR experiments were performed at magnetic field 4.7 T on a home-built broadband spectrometer operating in the frequency range 5–800 MHz. An Oxford 1200CF continuous flow cryostat was employed for measurements in the temperature range 3–300 K. Spectra were acquired by the spin-echo point-by-point method while varying the frequency, because of the large spectral width of the resonance lines. Correction of the line shapes has been made, by taking into account the ω^2 dependence of the signal intensity on frequency. Signal intensities at various temperatures were corrected by considering the spin-spin relaxation time T_2 and the Boltzmann factor at each temperature.

Figure 2 shows ^{139}La NMR line shapes for LCMO with $x = 0.55$ and 0.63 in the temperature range 3–200 K. A striking similarity is observed between the simulations of Fig. 1 and the temperature evolution of the spectra in Fig. 2. For $80 \leq T \leq 200$ K the NMR spectra consist of a narrow

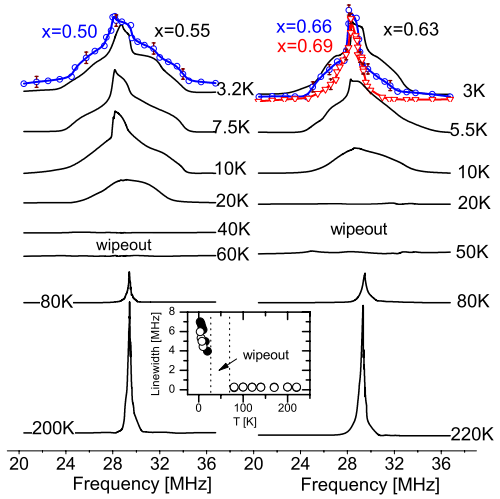

FIG. 2 (color online). ^{139}La NMR line shapes of the AFM signal as a function of temperature for $x = 0.55$ and 0.63. Spectra for $x = 0.50$ at 4 K (blue circles in left-hand panel) and $x = 0.66, 0.69$ at 3 K (blue circles and red triangles, respectively, in right-hand panel) are also presented. The inset shows the linewidth for $x = 0.55$ (●) and 0.63 (○) vs T.

symmetric line at frequency ≈29 MHz, which remains almost unshifted and without significant broadening by entering the AFM phase ($T_N \approx 150$ K). This is reminiscent of an AFM spin modulation that is commensurate with the underlying crystal lattice. Remarkably, for $T < T_N$ the signal intensity decreases rapidly by cooling and disappears at ≈60 K. This impressive wipeout effect is similar to the one observed in high T_c cuprates and nickelates [10,11], and will be discussed in more detail below. For $T \leq 30$ K a very broad spectrum reappears, which is characteristic of an IC modulation. By further decreasing the temperature the linewidth increases rapidly up to ≈7 MHz, as shown in the inset of Fig. 2. Unexpectedly, at low temperatures a relatively narrow peak emerges from the broad IC NMR signal, giving rise to spectra that closely resemble the spectrum in the upper right panel of Fig. 1. This strongly suggests that by lowering the temperature the IC modulation breaks into alternating commensurate and incommensurate regions giving rise to the particular soliton-modulated NMR signal. A similar temperature evolution of the NMR spectra was observed in LCMO $x =$ 0.50, 0.66, and 0.69. However, the IC modulation appears to reduce at higher doping values, as indicated by the narrowing of the IC NMR line shapes with increasing doping in Fig. 2. This is in conformity with electron diffraction experiments, which exhibit a decrease of the modulation wave vector according to the relation $q_s = (1 - x)a^\star$ [20].

Another distinguishing feature in Fig. 2 is the strong wipeout effect of the NMR signal, which takes place in the temperature range 30–60 K. The reason for the complete disappearance of the NMR signal is the extreme shortening of the spin-spin relaxation time T_2, as shown in Fig. 3. This makes part of the La nuclei relax so fast that the NMR signal decays before it can be measured. In general, the T_2 shortening by cooling is ascribed to slowing down of CDW or SDW fluctuations in accordance with relevant measurements in other systems [10,11,30]. Precursory effects by approaching the wipeout region are clearly seen in the T_1 vs T measurements (inset of Fig. 3). T_1 is observed to decrease by 1 order of magnitude when approaching the wipeout temperature region from above, and 2 orders of magnitude when approaching from below.

Of considerable interest is the $x = 0.5$ sample, which lies at the phase boundary of the T-x magnetic phase diagram, where coexistence of a relatively strong ferromagnetic (FM) phase component with the AFM phase is observed. By lowering the temperature this system undergoes a paramagnetic (PM) to FM phase transition at $T_c \approx 220$ K and a first order FM to AFM phase transition at $T_N \approx 180$ K by cooling (respectively, $T_N \approx 130$ K by heating) [34]. Electron [13] and neutron [34] diffraction experiments revealed the formation of a commensurate charge modulation for $T < T_N$, which becomes IC at higher temperatures. Figure 4 shows the evolution of the ^{139}La NMR signal from room temperature down to 3 K. At room temperature the PM NMR signal is located at ≈32 MHz. By lowering temperature, the NMR signal starts to shift at higher frequencies at ≈260 K, demonstrating the transition from the PM to the FM phase (the transition is shifted at higher temperatures in magnetic field 4.7 T). At temperatures lower than T_N the AFM signal component starts to grow at ≈29 MHz, which exhibits the same behavior as in all other studied samples; the narrow AFM NMR signal wipes out at ≈60 K, whereas a very broad IC signal reappears followed by a solitonic IC spectra at very low

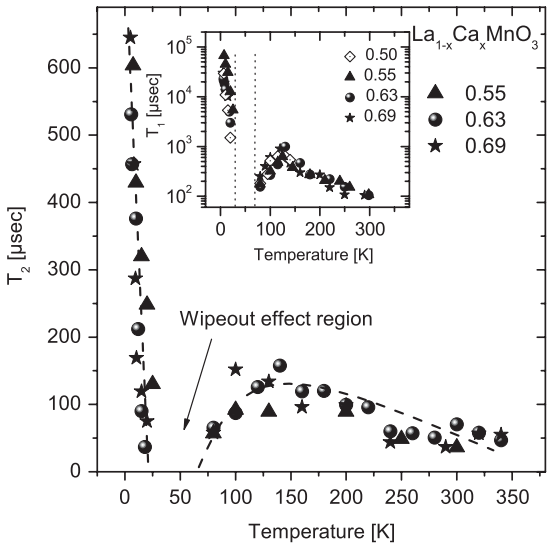

FIG. 3. ^{139}La NMR spin-spin relaxation time T_2 of the AFM signal as a function of temperature for LCMO $x = 0.55$, 0.63, and 0.69. In the temperature range 30–70 K the NMR signal disappears, due to extremely short T_2 values (wipeout). The inset shows ^{139}La NMR spin-lattice relaxation time T_1 vs T for $x =$ 0.50, 0.55, 0.63, and 0.69.

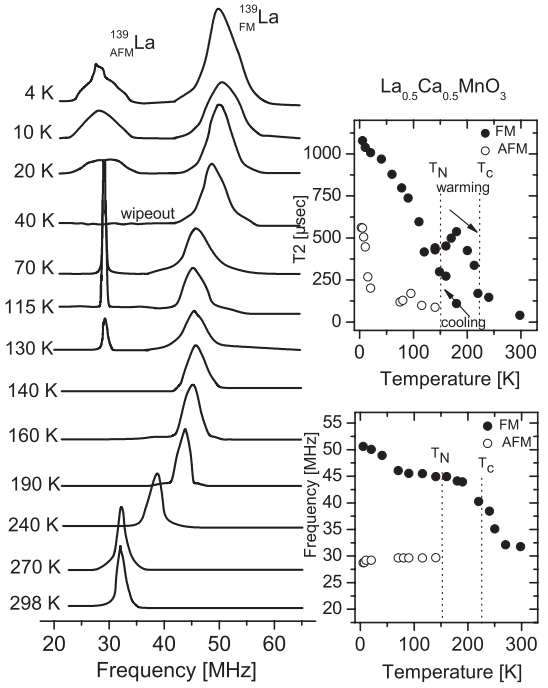

FIG. 4. ^{139}La NMR spectra for $x = 0.50$ at various temperatures. For $T < 70$ K the AFM signal component wipes out, while for $T < 30$ K the emerging broad IC NMR signal marks the appearance of an IC modulated AFM phase. The upper right-hand panel shows the spin-spin relaxation time T_2 vs T for both the FM and AFM signal components. The lower right-hand panel shows the corresponding signal frequencies.

temperatures. From the linewidth ≈ 7 MHz at 4 K, the amplitude ν_1 of the IC spin modulation can be estimated as $\nu_1 \approx 0.16\nu_{\mathrm{FM}}$, where $\nu_{\mathrm{FM}} \approx 22$ MHz is the frequency shift at 4 K of the fully polarized FM signal component from the Larmor frequency $\nu_L(4.7\ \mathrm{T}) = 28.26$ MHz. The upper right panel of Fig. 4 shows T_2 vs T. As expected, the T_2 of the FM signal component shows strong hysteresis between T_c and T_N. On the other hand, the T_2 of the AFM signal component exhibits the same behavior as in all other systems presented in Fig. 3. Another important remark is that the onset of the wipeout effect is accompanied by a strong frequency shift and significant broadening of the FM NMR signal. This indicates that the FM phase component does not consist of isolated FM islands embedded into an AFM matrix, but is rather strongly interacting with the AFM phase component.

In summary, our ^{139}La NMR measurements provide evidence that the ground state in overdoped LCMO manganites comprises an IC soliton-modulated SDW. At higher temperatures the modulation wave transforms to a uniform IC plane wave, which is subjected to strong slow fluctuations, as implied by the complete wipeout effect of the NMR signal. This is a completely new result, which urges us to reconsider our opinion about the low temperature electronic properties of overdoped manganites. Even more, the fundamental mechanism governing the establishment and evolution of the stripe phase appears to be common in overdoped manganites with cuprates and nickelates. In all these systems, charge order is established at higher temperatures than AFM order, while the growth of the IC modulation at low temperatures is accompanied by a strong wipeout of the NMR signal. Further experiments are needed in order to examine whether the solitonic ground state is a generic property of striped AFM transition metal oxide compounds.

Financial support by the Greek-German program IKYDA 2010 is acknowledged.

*Corresponding author.
gpapav@ims.demokritos.gr

[1] E. Dagotto, New J. Phys. **7**, 67 (2005).
[2] V. J. Emery, S. A. Kivelson, and J. M. Tranquada, Proc. Natl. Acad. Sci. U.S.A. **96**, 8814 (1999).
[3] J. M. Tranquada *et al.*, Nature (London) **375**, 561 (1995).
[4] J. M. Tranquada *et al.*, Phys. Rev. Lett. **73**, 1003 (1994).
[5] T. Hotta, A. Feiguin, and E. Dagotto, Phys. Rev. Lett. **86**, 4922 (2001).
[6] K. Machida, Physica (Amsterdam) **158C**, 192 (1989); M. Kato *et al.*, J. Phys. Soc. Jpn. **59**, 1047 (1990).
[7] J. Zaanen and O. Gunnarsson, Phys. Rev. B **40**, 7391 (1989).
[8] S.-W. Cheong *et al.*, Phys. Rev. Lett. **67**, 1791 (1991).
[9] S. M. Hayden *et al.*, Phys. Rev. Lett. **68**, 1061 (1992).
[10] A. W. Hunt *et al.*, Phys. Rev. Lett. **82**, 4300 (1999).
[11] N. J. Curro *et al.*, Phys. Rev. Lett. **85**, 642 (2000).
[12] M.-H. Julien *et al.*, Phys. Rev. B **63**, 144508 (2001).
[13] C. H. Chen and S.-W. Cheong, Phys. Rev. Lett. **76**, 4042 (1996).
[14] C. H. Chen, S.-W. Cheong, and H. Y. Hwang, J. Appl. Phys. **81**, 4326 (1997).
[15] S. Mori, C. H. Chen, and S.-W. Cheong, Nature (London) **392**, 473 (1998).
[16] G. Subias *et al.*, Phys. Rev. B **56**, 8183 (1997).
[17] J. Herrero-Martin *et al.*, Phys. Rev. B **70**, 024408 (2004).
[18] W. Luo *et al.*, Phys. Rev. Lett. **99**, 036402 (2007).
[19] W. Luo *et al.*, Phys. Rev. B **79**, 052405 (2009).
[20] J. C. Loudon *et al.*, Phys. Rev. Lett. **94**, 097202 (2005).
[21] A. Nucara *et al.*, Phys. Rev. Lett. **101**, 066407 (2008).
[22] G. C. Milward, M. J. Calderon, and P. B. Littlewood, Nature (London) **433**, 607 (2005).
[23] S. Cox *et al.*, Nature Mater. **7**, 25 (2008).
[24] N. D. Mathur and P. B. Littlewood, Solid State Commun. **119**, 271 (2001).
[25] L. Brey, Phys. Rev. Lett. **92**, 127202 (2004).
[26] L. Brey and P. B. Littlewood, Phys. Rev. Lett. **95**, 117205 (2005).
[27] R. Blinc, Phys. Rep. **79**, 331 (1981).
[28] C. Berthier *et al.*, Solid State Commun. **57**, 611 (1986).
[29] T. Takahashi *et al.*, J. Phys. Soc. Jpn. **55**, 1364 (1986).
[30] G. Papavassiliou *et al.*, Phys. Rev. Lett. **87**, 177204 (2001).
[31] M. J. Rice *et al.*, Phys. Rev. Lett. **36**, 432 (1976).
[32] B. Horovitz and J. A. Krumhansl, Solid State Commun. **26**, 81 (1978).
[33] B. Horovitz, Phys. Rev. Lett. **48**, 1416 (1982).
[34] P. G. Radaelli *et al.*, Phys. Rev. Lett. **75**, 4488 (1995).